

Towards ductile single-step polyelectrolyte complex films by means of plasticization

Jiaying Li^a, Sophie van Lange^d, Ameya Krishna B^a, Anastasia Athanasiadou^d, Gerard van Ewijk^b, Derk Jan van Dijken^c, Jasper van der Gucht^d, Wiebe M. de Vos^{a,*}

^a Membrane Science and Technology, MESA+ Institute for Nanotechnology, Faculty of Science and Technology, University of Twente, P.O. Box 217, 7500 AE Enschede, the Netherlands

^b AkzoNobel, Decorative Coatings bv, Rijksweg 31, 2171 AJ Sassenheim, the Netherlands

^c BASF Nederland B.V., Innovatielaan 1, 8447 SN Heerenveen, the Netherlands

^d Physical Chemistry and Soft Matter, Wageningen University and Research, 6708 WE Wageningen, the Netherlands

ARTICLE INFO

Keywords:

Polyelectrolyte complexation
Waterborne coatings
Plasticizer
Mechanical properties

ABSTRACT

Polyelectrolyte complexes (PECs) show great promise as functional coatings, including as oxygen barrier coatings for food packaging, but the brittleness of dry PECs limits their application. In this work, the possibility of plasticizing polyethylenimine/poly(4-styrenesulfonic acid) (PEI/PSS) films was investigated. Three different classes of plasticizers were chosen: salt, polyols, and ionic liquids (ILs). They were successfully incorporated in the evaporation-based single-step method. Potassium bromide or sorbitol plasticized films all showed crystallization upon evaporation, while films plasticized by glycerol, polyethylene glycol, and imidazole-based ILs all showed a clear brittle-to-ductile transition in their mechanical properties. The hydrophilicity of polyols and the amphiphilicity of these ILs allowed them to form homogenous casting solutions, but also increased their water sensitivity. The ionic nature of ILs make them more efficient as plasticizers since they can replace part of the PE-PE ionic-crosslinks, resulting in a more flexible network. Overall, this work demonstrates that ductile PEC films can be formed in a single step with controlled mechanical properties through plasticization.

1. Introduction

Polyelectrolytes are charged polymers that are typically soluble in water, but when brought together with oppositely charged polyelectrolytes they can form insoluble complexes. The exact nature of these formed polyelectrolyte complexes can be controlled by parameters such as the salinity and pH of the aqueous phase, but also by the polyelectrolyte type, molecular weight, charge density, and charge ratio [1]. This complexation process is governed by the formation of reversible ionic interactions between oppositely charged polyelectrolytes. In turn, reversible crosslinking facilitates the making of functional polyelectrolyte coatings, for example, that demonstrate oxygen barrier properties, with the possibility of recycling [2,3]. A major remaining challenge is the brittleness of polyelectrolyte complexes (PECs) when they are in their dense and dry form, caused by the rigid ionic crosslinking network [4,5]. To resolve this issue and increase the processibility of PECs, water and salt have been studied as plasticizers [6,7]. Water as the solvent of polyelectrolytes has a strong plasticizing effect

on PECs, as it can penetrate between the chains and disrupt polymer-polymer interactions, thereby also increasing the free volume [8–10]. As a result, dry PECs become more elastic when increasing the water content [11] and hydrated PECs show glass transitions which are not observed for dry PECs [12,13].

Salt plays an important role in polyelectrolyte complexation. As shown in Eq. 1 [4], the release of counterions (A^- and B^+) provides an entropy gain, which drives complexation (Pol^+Pol^-), while doping the complexes with a sufficiently high concentration of salt disrupts the structure of PECs [4,14].



Indeed, an increase in salt concentration gradually shifts the favorable state from intrinsic charge compensation dominated (Pol^+Pol^-) to extrinsic compensation dominated (Pol^+A^- and Pol^-B^+) by charge screening [15]. The concentration of required salt is determined by the exact nature of the polyelectrolytes and the type of salt, where KBr is one of the most studied salts that shows effective, strong doping [16].

* Corresponding author.

E-mail address: w.m.devos@utwente.nl (W.M. de Vos).

<https://doi.org/10.1016/j.porgcoat.2023.107459>

Received 18 November 2022; Received in revised form 25 January 2023; Accepted 31 January 2023

Available online 7 February 2023

0300-9440/© 2023 The Author(s). Published by Elsevier B.V. This is an open access article under the CC BY license (<http://creativecommons.org/licenses/by/4.0/>).

With the aid of aqueous salt solutions, PECs can be softened and processed in a way that is analogous to the use of temperature to process thermoplastics. For this reason, the term “saloplastics” was coined [6]. However, using salt to control PEC properties is often tied to water absorption and a combined effect of both salt and water is observed. Salt, on one hand, can weaken the ionic interaction between Pol^+Pol^- and thus increase the mobility of the chains, while on the other hand it can compete with the PEC for water [17]. This dual effect of salt depends on the hydration level, which becomes critical for dry PEC coatings. In our previous work [3,18], salt crystallization was observed when evaporation was used for film formation. The strong driving force of A^- and B^+ to form salt crystals AB reduces the effect of salt on the equilibrium in Eq. 1.

Stepping away from water and salt, polyols have successfully been used as plasticizers for single polyelectrolytes. For food packaging applications, these small molecules, including glycerol, poly(ethylene glycol), and sorbitol, have been studied for plasticizing bio-based polyelectrolyte films such as chitosan derivatives, alginates, and their complexes [19–29]. Their plasticizing functionality is similar to that of water, with an additional benefit of non-volatility. Although they have attracted enormous interest as plasticizers in standard coatings, they have not been systematically studied for PECs. One reason for this may be the difficulty to incorporate them during PEC formation since most PECs are prepared by layer-by-layer (LbL) deposition or extrusion [30,31]. Another reason is that PECs are mainly used in their hydrated state, where water already serves as a plasticizer, for example, in membranes [32]. However, other plasticizers become relevant for coatings where the humidity of the environment can be low.

Other potential plasticizers for PECs are ionic liquids (ILs). These organic salts have low melting temperatures and low volatility, which may provide other unique functionalities, such as ionic conductivity [33–40]. Most of these plasticizing ILs have alkyl-imidazolium-based cations and inorganic anions, for example, 1-butyl-3-methylimidazolium chloride (BMIMCl). These specific combinations of cations and anions allow these ILs to become amphiphilic and they have shown successful plasticization of many carbohydrates, such as cellulose, starch, and chitin-based materials [33,38,41–44]. ILs have also been shown to successfully swell/plasticize PECs [45–47]. Zhang et al. showed that the larger and more hydrophobic cation BMIM⁺ binds stronger than Na⁺ and creates more plasticization [47]. The use of ILs as plasticizers for PECs should have the advantages of both water and salt as they not only increase the chain mobility but also weaken the ionic interaction between the polyelectrolytes.

In our previous work, we have studied the mechanical properties of PEI/PSS complex films, which showed high Young's moduli and limited extensibility. This overall brittleness was mainly a result of the high ionic crosslinking density, which is beneficial for minimizing swelling. However, their brittleness hinders the practical use of these PEC films. To better control the mechanical properties of PEI/PSS complexes, here we study the effects of several plasticizers with different natures and interaction strengths. We incorporate polyols, salt, and ILs into the films using a single-step solution mixing and casting approach. The resulting films were characterized to investigate how these plasticizers influence the film appearance, flexibility, and water sensitivity. Overall, we show that different types of plasticizers can plasticize PECs via various mechanisms, allowing a great deal of extra control over the mechanical properties of PEC films and coatings.

2. Experimental section

2.1. Materials

Branched polyethylenimine (PEI, average M_w 25 $\text{kg}\cdot\text{mol}^{-1}$, ≤ 1 % water), poly(4-styrenesulfonic acid) (PSS, average M_w 75 $\text{kg}\cdot\text{mol}^{-1}$, 18 wt% in water), ammonia (NH_3 , for analysis EMSURE® ISO, Reag. Ph Eur, 25 % in water), glycerol (GLY, puriss., meets analytical

specification of Ph. Eur., BP, USP, FCC, E422, anhydrous, 99.0–101.0 % alkalimetric), polyethylene glycol 200 (PEG, M_w 200 $\text{g}\cdot\text{mol}^{-1}$, for synthesis), D-sorbitol (SOR, ≥ 98 %), potassium hexafluorophosphate (KPF_6 , ≥ 99 %), 1-ethyl-3-methylimidazolium bromide (EMIMBr, ≥ 97.0 %), 1-butyl-3-methylimidazolium bromide (BMIMBr, > 97.0 % HPLC), and 1-butyl-3-methylimidazolium hexafluorophosphate (BMIMPF₆, ≥ 97.0 % HPLC) were all purchased from Sigma-Aldrich (The Netherlands). 1-Methyl-3-octylimidazolium bromide (OMIMBr, 99 %) was purchased from Iolitec, Germany. All chemicals were used without further purification. All water used was deionized water (Milli-Q®, Merck, The Netherlands). Acetate sheets (250 μm thick) were purchased from JEJE produkt, The Netherlands.

2.2. Preparation of PEI/PSS/plasticizer solutions

PSS as a solid was obtained by drying the obtained solution as small pellets at 60 °C for 2 h and they were then stored at 30 °C under vacuum. A 25 wt% PSS solution was then prepared by diluting the PSS solid with ammonia and water (PSS: NH_3 wt% ratio 1:0.53). A 25 wt% PEI solution was prepared by diluting the stock solution. The standard 25 wt% PEI:PSS solution was prepared at a ratio of 2:1, this ratio was selected based on previous work where this ratio showed the lowest degree of swelling [18]. This mixing ratio describes the molar charged monomer ratio ($M_{EI} = 43.04 \text{ g}\cdot\text{mol}^{-1}$ and $M_{SS} = 184.23 \text{ g}\cdot\text{mol}^{-1}$).

Different concentrations of selected plasticizers were investigated. Their chemical structures are shown in Fig. 1. For all plasticizers, the studied range was 2.0 to 10.0 wt% on total solution (Table 1). For all mixtures, PEI:PSS was maintained at a ratio of 2:1 and 25 wt%. To make the mixture, plasticizer was first added into 50 wt% PEI solution. Then, 25 wt% of PSS- NH_3 was added. In the end, water was added to obtain the desired overall concentration. All mixtures were stirred overnight and allowed to degas. Assuming that water and ammonia fully evaporate, the final composition of all dried mixtures are shown in Table 1. When phase separation was observed in solution, it was not further used for casting.

2.3. Film fabrication and thickness control

A BYK automatic film applicator (USA) was used for casting. Three different thicknesses were studied first (gap height 50, 100, and 200 μm). With acetate sheet as substrate, free-standing films could be removed from the substrate. The final thickness of each film was the difference between the thicknesses of coated and uncoated areas measured by a micrometer. The average result of 10 random points with standard deviation is reported. When the films showed no cracking at these thicknesses, thicker films were gradually prepared (from gap height 300 μm up to 800 μm) in order to find the critical cracking thickness, which is defined as the maximum value beyond which films crack [48].

2.4. Film characterizations

2.4.1. 3-point bending

A 3-point bending test (Instron 5942, USA) was utilized to examine the flexibility of the coating layer at low thicknesses. A PEI/PSS coated acetate sheet was cut into 2 cm \times 4 cm strips and loaded with a support span $l = 2$ cm. The coated side was facing downwards. The loading velocity was 20 mm/min and the punch was set to travel 12 mm. For all samples, the maximum force applied was around 2 N and the maximum stress was around 56 MPa. Images of the 3-point bending experimental set-up are shown in Fig. S1. The flexure modulus and strain of the blank acetate sheet were around 3880 MPa and 3 %. However, the final modulus of the samples coated with the thin PEC films was dominated by the bulk substrate and no significant differences could be observed after adding the coating. Thus, we only used this method to observe cracking of the films after bending. The measurements were conducted

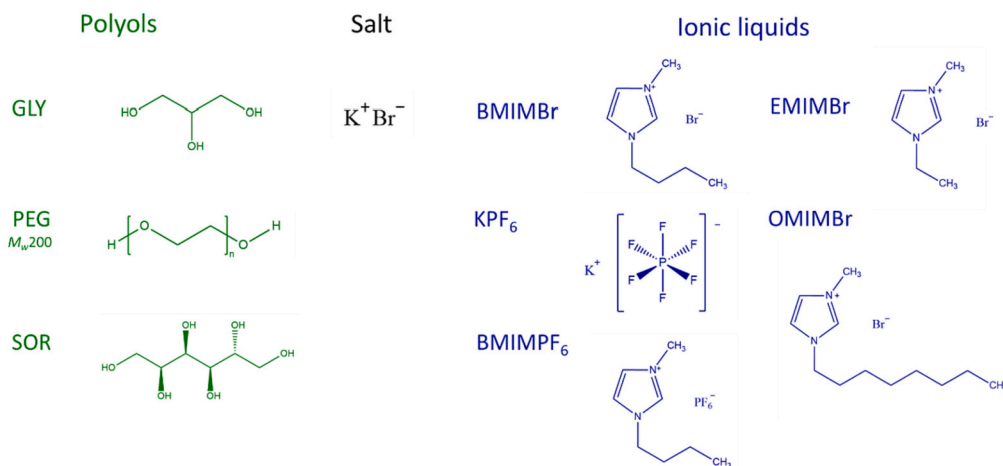


Fig. 1. Chemical structures of studied plasticizers in three classifications: polyols, salt, and ILs.

Table 1

Different types and concentrations of plasticizers studied in PEI:PSS and their wet/dry compositions.

PEC in solution	Plasticizer wt% in solution	PEC dry wt %	Plasticizer dry wt %
25 wt% PEI:PSS 2:1	2.0	92.6	7.4
	4.0	86.2	13.8
	6.0	80.6	19.4
	8.0	75.8	24.2
	10.0	71.4	28.6

under ambient conditions where the temperature (T) was 18.8–19.4 °C and relative humidity (RH) was 46–50 %. After the 3-point bending tests, the film appearance and cracking were examined by an optical microscope (Leitz Ortholux, Germany).

2.4.2. Opacity

The opacity of each film (except for cracked films) was determined by a UV spectrophotometer (UV-1800 Shimadzu). The sample was cut into a 0.9 cm × 3.2 cm rectangular shape and placed perpendicularly into a polystyrene cuvette. A piece of uncoated acetate sheet was cut to the same size, placed in the same position, and used as background. The absorbance at wavelength 600 nm was recorded and for every film composition, 3 samples were measured and the average results were reported, including the standard deviations. The film opacity is defined as the light absorbance (Abs_{600}) at 600 nm over the film thickness d (mm) as shown in Eq. 2:

$$\text{Opacity (mm}^{-1}\text{)} = \frac{Abs_{600}}{d} \quad (2)$$

2.4.3. FTIR

Fourier transform infrared spectroscopy (FTIR, Spectrum two, PerkinElmer, USA) was utilized to compare blank and plasticized films (gap height 200 μm). The reflectance mode was used at a spectral resolution of 4 cm⁻¹ from wavenumber 400 cm⁻¹ to 4000 cm⁻¹. 16 scans were performed for each measurement. The temperature was 19 °C and RH was 50 %.

2.4.4. Water content and water uptake

The water content and water uptake of free-standing samples (gap height 300 μm samples) were measured. The water content (%) was calculated based on Eq. 3:

$$\text{Water content (\%)} = \frac{m_{\text{ambient}} - m_{\text{dry}}}{m_{\text{ambient}}} * 100 \quad (3)$$

where m_{ambient} is the weighed mass under ambient conditions (T 19 °C, RH 48–51 %) and m_{dry} is the weighed mass after drying at 80 °C for 4 h and storing under vacuum at 30 °C overnight.

For water uptake, a 0.5 g sample was added to deionized water (50 mL) and stirred by a stirring bar for 1 h. After 24 h soaking, extra surface water was removed carefully with dust-free tissues and the wet weight of 3 different sets was measured. Then, the sample was dried following the same procedure and the average result was reported. The water uptake (%) was calculated according to Eq. 4, with dry weight (m_{dry}) and wet weight (m_{wet}).

$$\text{Water uptake (\%)} = \frac{m_{\text{wet}} - m_{\text{dry}}}{m_{\text{dry}}} * 100 \quad (4)$$

During the swelling tests, it was observed that the films were partially dissolved and that PEs and plasticizers may be leached. A leaching test was conducted by first drying the samples in an oven at 80 °C for 4 h and then storing under vacuum at 30 °C overnight, after which the initial dry weight m_{before} was obtained. Secondly, the dry samples were soaked in water for 24 h, then each sample was rinsed thoroughly. Last, the rinsed samples were dried again following the same procedures to obtain m_{after} . The leached wt% can be calculated as shown in Eq. 5:

$$\text{Leached weight (\%)} = \frac{m_{\text{before}} - m_{\text{after}}}{m_{\text{before}}} * 100 \quad (5)$$

2.4.5. TGA

To study the decomposition behavior vs concentration of different plasticizers, thermogravimetric analysis (TGA, NETZSCH, STA 449 F3 Jupiter®, USA) was conducted at 40–800 °C with a ramp of 10 °C/min under a nitrogen environment. Heating was maintained for 5 min after reaching 800 °C then followed by cooling. For measuring the water content of blank PEI/PSS and GLY plasticized samples, the temperature range was set to 30–120 °C (5 °C/min) and maintained for 20 min. For each reported value, 3 measurements were conducted.

2.4.6. SEM

To examine whether the films were dense, scanning electron microscopy (SEM, JSM-6010LA, JEOL, Japan) was used. The samples (gap height 300 μm) were stored under vacuum overnight at 30 °C to remove excess water and coated with a Pt/Pd 5 nm coating (Quorum Q150T ES, Quorum Technologies, Ltd., UK).

2.4.7. Tensile measurements

When free-standing films of sufficient thickness could be successfully prepared, tensile measurements (Instron 5942, USA) were performed to

study their mechanical properties. After drying under ambient conditions (>72 h), 5 cm × 0.5 cm (height × width) strips of samples were cut and then carefully lifted from the substrate with a tweezer. The thickness of each sample was determined by a micrometer at 4 random points. For tensile measurements, the preparation of the blank sample was not possible because PEI:PSS was too brittle at a ratio of 2:1. Samples plasticized by GLY, PEG, EMIMBr, or OMIMBr were prepared at gap height 300 μm. For BMIMBr, samples were cast at both gap heights of 300 and 800 μm. The studied concentrations of plasticizers varied and the maximum concentration used was the one where the film became too soft to handle. For each data point, at least 3 samples from different films were measured and the testing speed was 1 mm•min⁻¹. The ambient conditions were RH 42–44 % and T 19.3–19.6 °C.

2.4.8. DMA

To examine the mechanical properties as a function of the relative humidity, dynamic mechanical analysis (DMA) was performed on a TA Q800 instrument in film tension mode with a custom relative humidity control unit. 30 wt% PEI:PSS at a ratio of 3:1 was used as the blank sample without plasticizer since the 2:1 sample was too brittle for successful sample loading. As the comparison, 30 wt% PEI:PSS at a ratio of 3:1 was doped with 4 wt% BMIMBr. The final dry sample consisted of around 88 wt% PEI/PSS and 12 wt% BMIMBr. Both solutions were cast with a 1.5 mm casting bar. Dry rectangular samples (2 cm × 0.5 cm) were used to determine the linear viscoelastic regime by performing an amplitude sweep. The evolution of the modulus while equilibrating to various relative humidity was monitored in oscillatory mode with a frequency of 1 Hz and an amplitude of 0.01 for undoped and 0.1 % for doped samples. The temperature was around 21 °C.

3. Results and discussion

3.1. Formation of homogeneous solutions

The first requirement to prepare PEC coatings using our previously developed one-step casting method, is to make homogenous solutions containing both polyelectrolytes and the plasticizer. One of the key parameters for selecting a suitable plasticizer for PECs is its hydrophilicity. As shown in Fig. S2a–d, all solutions with polyols (GLY, PEG, and SOR) and KBr were homogenous and no phase separation was observed within the studied range. For ILs, we first compared BMIMBr, KPF₆, and BMIMPF₆, which have decreasing solubilities in water. BMIMBr is miscible in water, while KPF₆ has a lower water solubility (around 8.4 wt% at 25 °C) [49], and the solubility of BMIMPF₆ is the lowest (around 2.4 wt% at 303 K) [50]. As shown in Fig. S2e–f, the mixtures with BMIMBr and KPF₆ all appeared homogenous. For BMIMPF₆, the mixtures appeared homogenous up to 6 wt% (Fig. S2g), while both samples with 8 and 10 wt% BMIMPF₆ showed phase separation, leading to droplets of BMIMPF₆ at the bottom of the vials (Fig. S2h). Therefore, these two samples were not used for casting. We also tried two other ILs, EMIMBr and OMIMBr, which differ from BMIMBr in the length of the imidazolium alkyl chain length. Homogeneous solutions were also successfully prepared (Fig. S2i and S2j).

3.2. Film appearance

All solutions were cast first with gap heights of 50, 100, and 200 μm. If plasticized films remained intact up to gap height of 200 μm, thicker films were prepared (300, 400, 500, and 800 μm). Potassium bromide (KBr) was chosen as the plasticizing salt due to its well-studied plasticizing behavior with PECs [16,51]. During the preparation of 2–10 wt% KBr films, crystallization was observed, thus a narrower range 1–5 wt% was studied. Crystallization was observed for films with 2 wt% KBr at 200 μm gap height and for all films of ≥3 wt% KBr (Fig. S3). At least 10.98 wt% KBr would be required to achieve full extrinsic compensation of the polymeric charges (see in Calculation S1). However, salt

crystallization happened at much lower concentration, which indicates that only limited extrinsic compensation can occur. Therefore, using salt alone as plasticizer is not a suitable approach for evaporation-based film formation.

Selected polyols, glycerol (GLY), polyethylene glycol (PEG), and sorbitol (SOR), all successfully led to the formation of coatings. However, SOR failed to remain in the films. When the concentration was ≥4 wt%, white crystals were observed in these films by eye and optical microscopy (Fig. S4), indicating that SOR did not stay homogeneously mixed during drying and similar to KBr, crystallization happened. All GLY and PEG plasticized films appeared homogenous and with concentration 8/10 wt%, thicker films can also be cast. When the dry thickness exceeded 50 μm, however, a wrinkling of the films was observed for both plasticizers. As shown in Fig. S5, the increase of thickness and concentration of plasticizer created larger wrinkles. A possible explanation for the wrinkling is the formation of a skin layer. The PEI/PSS complexes form first at the air/film interface, where the polymer concentration is highest as a consequence of the moving evaporation front. For thick films, the concentration gradients may become so large that the top layer becomes rigid while the bulk is still mobile. As evaporation continues and the bulk volume decreases, wrinkles develop [52,53]. Due to this wrinkling, only samples made with gap height of 300 μm are used for further tensile tests.

We then considered the addition of ionic liquids as plasticizer. Similar to KBr and SOR, both KPF₆ and BMIMPF₆ showed phase separation during drying. For KPF₆, crystallization was observed for initial concentrations higher than 6 wt% (Fig. S6a), while for BMIMPF₆, small droplets were trapped in the film from 4 wt% onwards (Fig. S6b). This suggests that mixing BMIMPF₆ into the system leads to emulsions instead of homogenous solutions. By contrast, BMIMBr showed good compatibility. Some small demixing spots were observed as shown in Fig. S7a, however, overall the films appeared homogenous. It was observed that when the relative humidity exceeded 70 %, the films showed more demixing areas and shrunk in general (Fig. S7b and c). Thicker films showed more demixing. Compared to GLY and PEG, there was no wrinkling at higher thickness. The ionic interaction between ILs and PEI/PSS allowed the whole ionic crosslinking network to remain flexible, which may reduce the effect of drying stresses and skin formation on the morphology of the films.

For both EMIMBr and OMIMBr, no homogeneous films could be obtained. As shown in Fig. S8a, the addition of EMIMBr increased the film mobility and hydrophilicity. For 2 and 4 wt%, the films shrunk and dewetted, while above 4 wt%, the films remained liquid-like. On the other hand, OMIMBr has bulkier side chains which are more hydrophobic. This created localized demixing defects which escalated with increasing the concentration (Fig. S8b). In both cases, changing acetate sheets to more hydrophilic or hydrophobic substrates showed no improvements (Fig. S9), showing that these effects were not substrate dependent.

Next, FTIR was used to examine the film composition. Here, films that showed crystallization were not measured since phase separation occurred, making the FTIR results difficult to interpret. Plasticizers were successfully embedded in the films and the spectra were in line with increasing amounts of plasticizers (Figs. S10, S11, and S12). It was noticed that above a critical concentration (GLY 8 wt%, PEG 10 wt%, EMIMBr 6 wt%, BMIMBr 8 wt%, OMIMBr 10 wt%), films would become sticky and liquid-like. Compared to literature, much more wt% of polyols can be added (up to 40 wt%) into chitosan and its blend materials than to our PEC [24,54–58]. The possible reason may be that the high degree of ionic crosslinking of PEI/PSS results in much less free volume, so that smaller amount of polyols can be added.

Furthermore, SEM was used to check the morphology of free-standing films (Fig. S13). All films appeared smooth and, at high magnification, no pore structure was observed. To further rule out the formation of pores, we checked the transparency of the films, which is an important characteristic of a coating and provides some insight about

the overall homogeneity. Films that were cracked after drying were not measured because the cracks would influence the results. The opacity of the bare acetate sheet was $0.23 \pm 0.01 \text{ mm}^{-1}$, while the blank PSS/PEI film has an opacity of $2.21 \pm 1.77 \text{ mm}^{-1}$. Adding KBr at concentrations $\leq 3 \text{ wt}\%$ led to improved transparency, because it improves the mobility of chains and helps the film formation (Fig. 2a). However, when increasing the wt%, crystallization started to happen especially for thicker films, leading to higher opacity. For SOR, crystallization produced rather inhomogeneous films, even at low concentrations, leading to a much higher opacity than the blank (Fig. 2b). For both GLY and PEG, we see that the addition of plasticizer first introduces heterogeneity in the films, while further increasing the concentration makes the films more transparent. At low plasticizer concentration, increasing the

thickness reduced the opacity. This may be because thinner films were more difficult to cast at these high viscosities, which may lead to stripes, due to poor leveling. At high plasticizer concentration (10 wt%), the films were less viscous so that better leveling was obtained. In this case, the opacity increases with thickness, possibly because the extra plasticizer may increase the heterogeneity. Overall, GLY plasticized films showed lower opacity than PEG plasticized films.

Among all plasticizers, BMIMBr plasticized films showed the lowest opacity (Fig. 2e). In general, all films showed undetectable opacity unless some small demixing defects were present. This indicates good compatibility of BMIMBr with PEI/PSS. KPF₆ and BMIMPF₆ plasticized films showed similar trends to KBr and SOR, because of phase separation (Fig. S14). Films plasticized by EMIMBr and OMIMBr showed severe

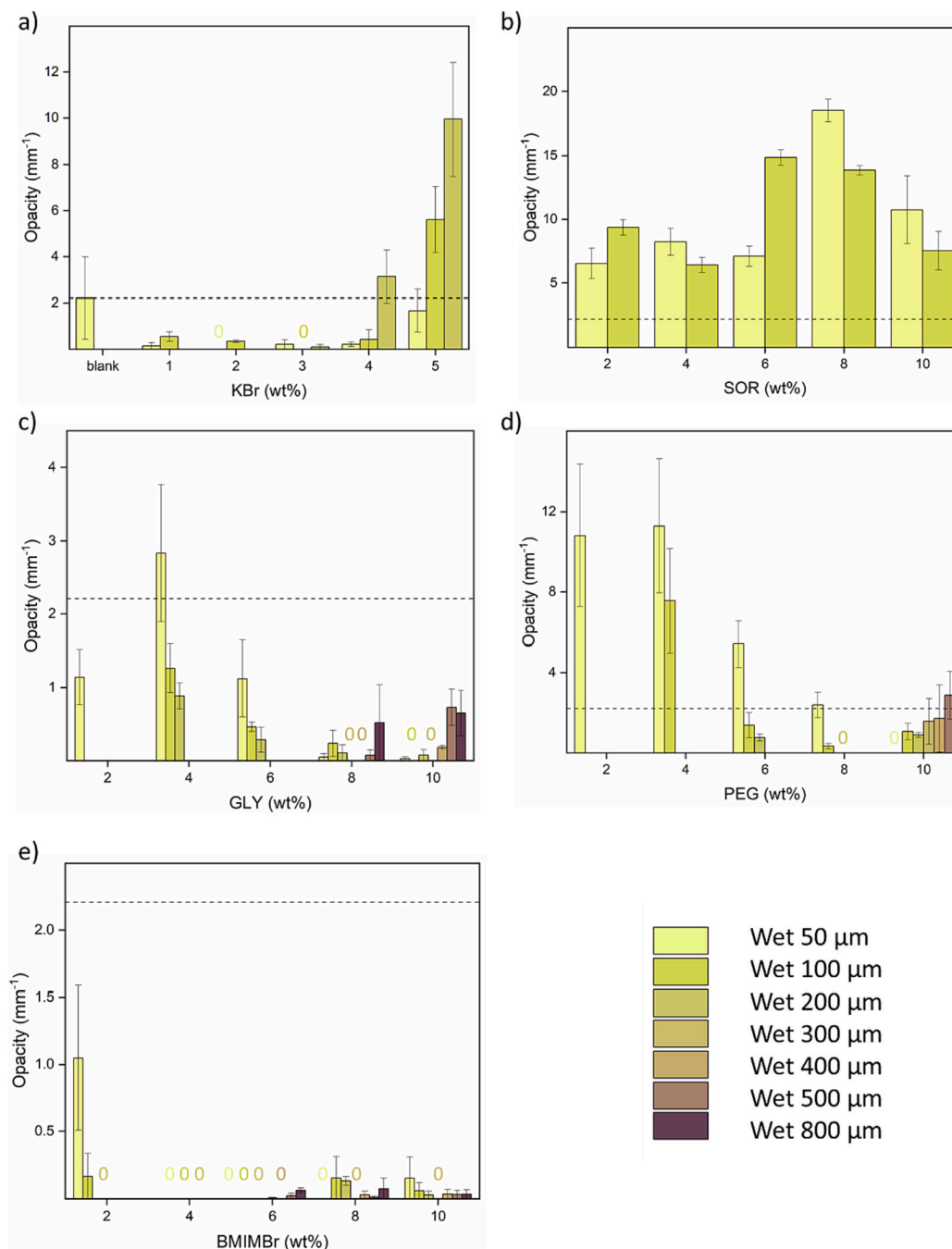


Fig. 2. Opacity of films plasticized by a) KBr, b) SOR, c) GLY, d) PEG, and e) BMIMBr. Error bars indicate the standard deviation and dashed lines indicate the average opacity of the blank. 0 here means no difference was detected between bare substrate and the coated samples.

demixing, yet did not affect the transparency.

3.3. Water content and leaching

As shown in Fig. 3a and b, the addition of hydrophilic plasticizers gradually increased the water content and uptake of the films. All plasticizers showed similar results. The water content of blank and GLY samples was also measured by TGA (Fig. S15), and the same trend was observed. While performing the swelling tests, it was noticed that some of the films were partially dissolving. Possibly, PEs and plasticizers can gain mobility in water and might be leached from the films. Thus, the water uptake experiments were no longer reliable (Fig. S16). Instead, leaching tests were performed for some samples as shown in Figure 3b. The blank sample (PEI:PSS at a ratio of 2:1 without plasticizer) showed around 20 wt% leaching. Probably, the loosely-bound excess PEs gained mobility upon contact with water and dissolved in the water phase. For 8 wt% GLY and PEG plasticized samples, >40 wt% of the films was leached. As compared to the calculated dry wt% in Table 1, it indicated excess PEs and most of the plasticizer were released into water. By contrast, for 4 wt% IL plasticized samples, less plasticizer or/and polymer were leached. When increasing the concentration of BMIMBr to 8 wt%, there was more leaching, probably because the excess BMIMBr was not bound strongly. An interesting expansion phenomenon was observed for IL plasticized samples (Fig. S17). Instead of leaching into the water, the film expanded horizontally in water, but was still held together by ionic interactions. Two thicknesses (gap height 300 and 800 μm) of BMIMBr plasticized samples were compared in terms of water content, water uptake, and leaching (Fig. S18). There was no significant difference.

3.4. Thermal stability

The thermal stability of the blank and plasticized films are shown in Fig. 4. For GLY, the major mass loss starts around 200 $^{\circ}\text{C}$ and finishes at around 250 $^{\circ}\text{C}$ [59,60]. As a result, GLY plasticized films showed the lowest thermal stability (Fig. 4a). PEG is slightly more stable and decomposes between 200 and 350 $^{\circ}\text{C}$ (Fig. 4b) [61]. By contrast, ILs are more thermally stable. For all three, the onset decomposition temperature is around 280 $^{\circ}\text{C}$ and the major weight loss finishes around 320 $^{\circ}\text{C}$ [62–66]. Thus, ILs plasticized films did not show much decrease in thermal stability (Fig. 4c, d, and e). For all plasticizers, the increase of concentration led to lower thermal stability and less residual weight. At the same concentration of 4 wt%, the major decomposition peak for all plasticizers are compared (Fig. 4f). In this temperature range (300–460 $^{\circ}\text{C}$), most of the plasticizers should be fully decomposed. For polyols plasticized films, polyols first decomposed, then the major

decomposition of PEC started following the same trend as the blank. Polyols have limited influence on the ionic crosslinking between PEI and PSS since dipole-ionic interaction is weaker than ion-ion interaction. Thus, their peaks fall into the same region as the blank. By contrast, ILs interfere with the network of ionic crosslinking. Ionic interactions between PEI and PSS are partially replaced by PEI^+-Br^- and $\text{PSS}^--\text{BMIM}^+$. As a consequence, broader peaks were formed compared to the blank and the onset decomposition temperature was lowered.

3.5. Mechanical properties

3.5.1. 3-point bending of coated films

To examine the flexibility of the coating, 3-point bending measurements were performed. Based on our previous study [18], we chose PEI:PSS at a ratio of 2:1 as the starting point (referred to as Blank in this section), since it showed the strongest complexation and the least swelling. However, without plasticizer, the critical thickness at which cracking occurs in these films is low, so that only thin films could be prepared, which could not be removed from the substrate without damaging them. Thus, standard sized samples could not be prepared for tensile measurements. Rather than using free-standing films, we therefore carried out the 3-point bending tests directly on the coated substrates. Although this did not allow us to measure the modulus of the PEC film, we could observe the state of the film after bending it, by observing the possible formation of cracks using an optical microscope. We distinguish three different cases in the films that we studied. The most brittle films already cracked during drying, due to the build-up of stress during drying and the adhesion to the substrate. It is well-known that this depends on the thickness of the film, with cracking only occurring for films that are thicker than the critical cracking thickness [48]. Other films remained intact during drying, but showed cracks after the bending test. Finally, the strongest films remained intact and adhere to the substrate even after bending. This classification serves as a first assessment to help find the suitable plasticizers and their concentrations.

The state diagrams of plasticized films vs dry thickness are summarized in Fig. 5. As shown in Fig. 5a, blank PEI:PSS at a ratio 2:1 cracked during drying when the dry thickness exceeded 10 μm , while below 10 μm , the films cracked upon bending. KBr improved the mechanical strength of the films, in particular for higher salt concentrations which cracked after bending around 25 μm . With the gradual addition of GLY (Fig. 5b), the flexibility was significantly improved, with films remaining intact even at higher thicknesses when the GLY concentration was ≥ 8 wt% in solution (≥ 24.2 wt% in dry films). A similar trend was observed with PEG as shown in Fig. 5c. BMIMBr also showed effective plasticization at even lower concentrations (Fig. 5d). Compared to KBr plasticized films, films plasticized by GLY, PEG, and BMIMBr all showed

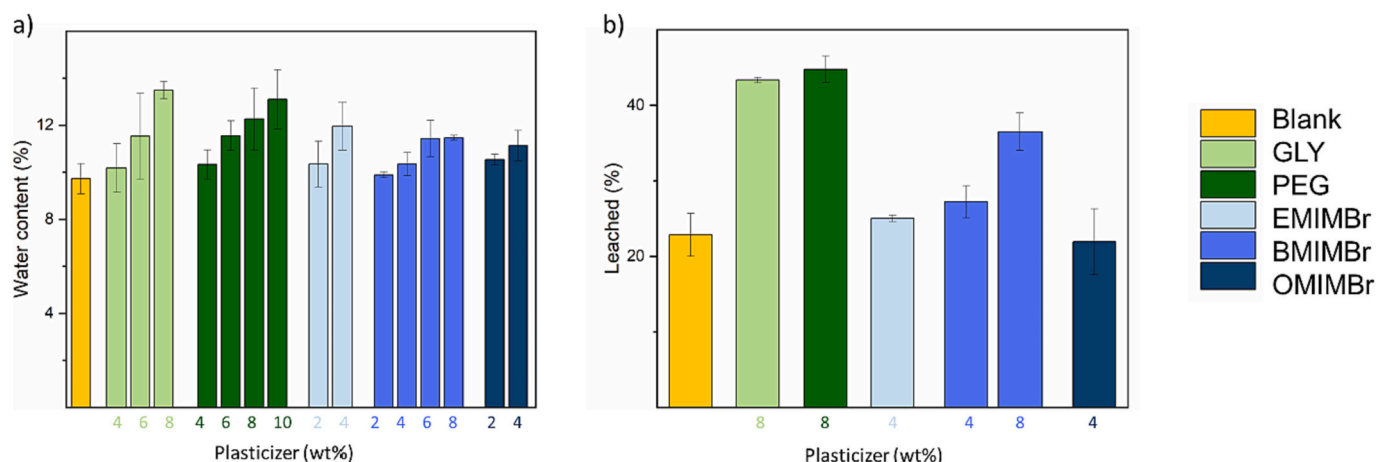


Fig. 3. a) Water content and b) leaching tests of plasticized samples and blank.

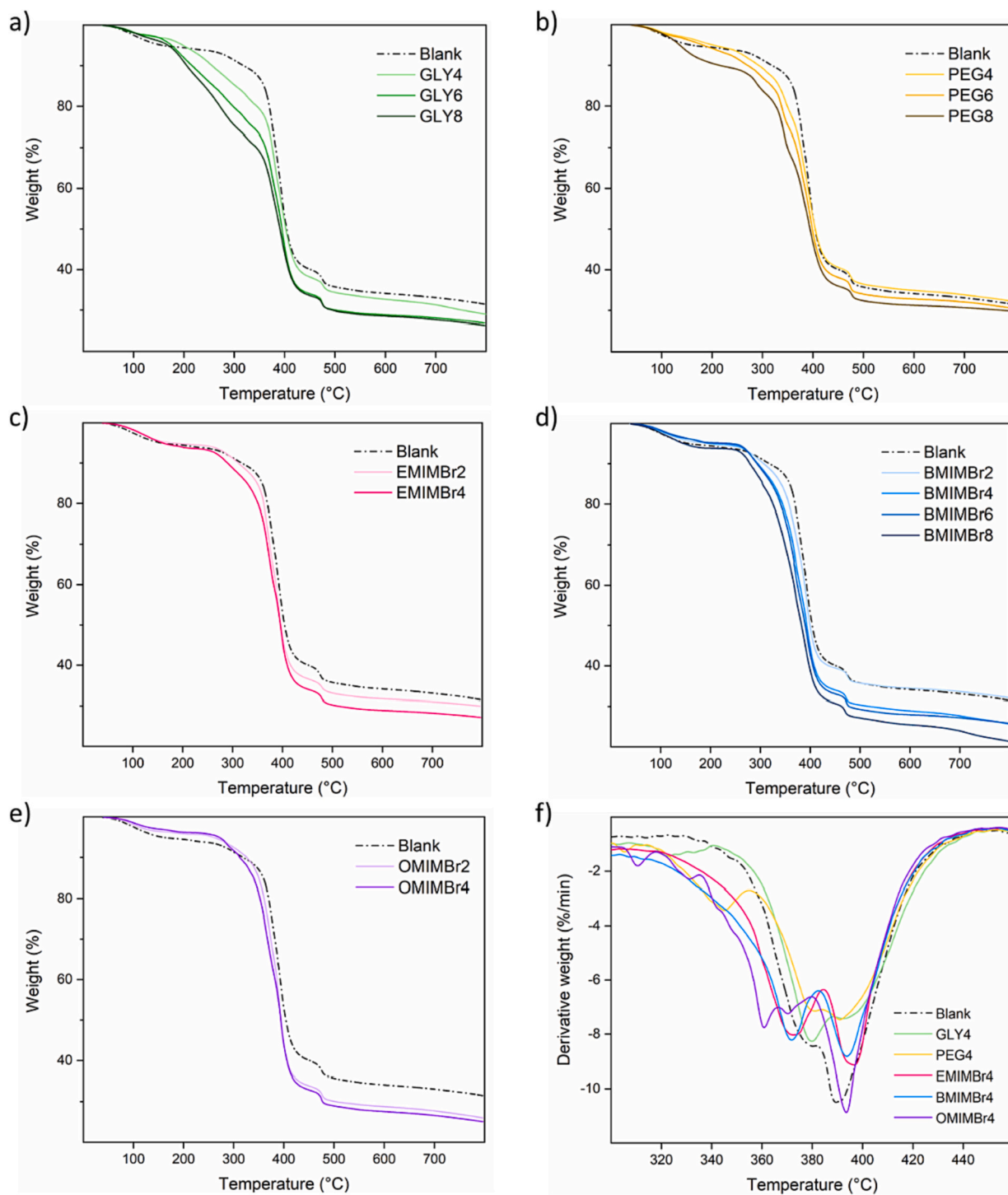


Fig. 4. TGA results of blank and films plasticized by different concentrations of a) GLY, b) PEG, c) EMIMBr, d) BMIMBr, and e) OMIMBr. f) Derivative weight vs temperature (300–460 °C) of 4 wt% plasticized samples.

an increase in critical thickness which indicates the plasticizers were successfully incorporated inside. Higher thicknesses were also prepared for GLY 8/10 wt%, PEG 8/10 wt%, and BMIMBr (6–10 wt%) plasticized films. Films plasticized by 10 wt% PEG cracked when the thickness exceeded 150 μm , while GLY 8/10 wt% plasticized films only showed microcracks near the edge (Fig. S19a). For BMIMBr, all films with concentration of 6 wt% or higher were intact up to a dry thickness around 160 μm , thus even outperforming GLY and PEG. SOR, KPF₆, and BMIMPF₆ all failed to plasticize the films since phase separation occurred (Fig. S19b, c, and d). All optical images of the films after

bending are summarized in Fig. S20.

3.5.2. Tensile measurements of free-standing films

Samples for tensile testing were prepared with the same gap height of 300 μm . The final dry thicknesses are shown in Table S1. In general, films showed higher thickness when increasing the concentration of plasticizers since the dry mass increased. Blank PEI:PSS at a ratio of 2:1 was too brittle to be measured. Samples with insufficient plasticizer concentrations could be prepared, however, they cracked during clamping. For EMIMBr, only 4 wt% was measured since above this

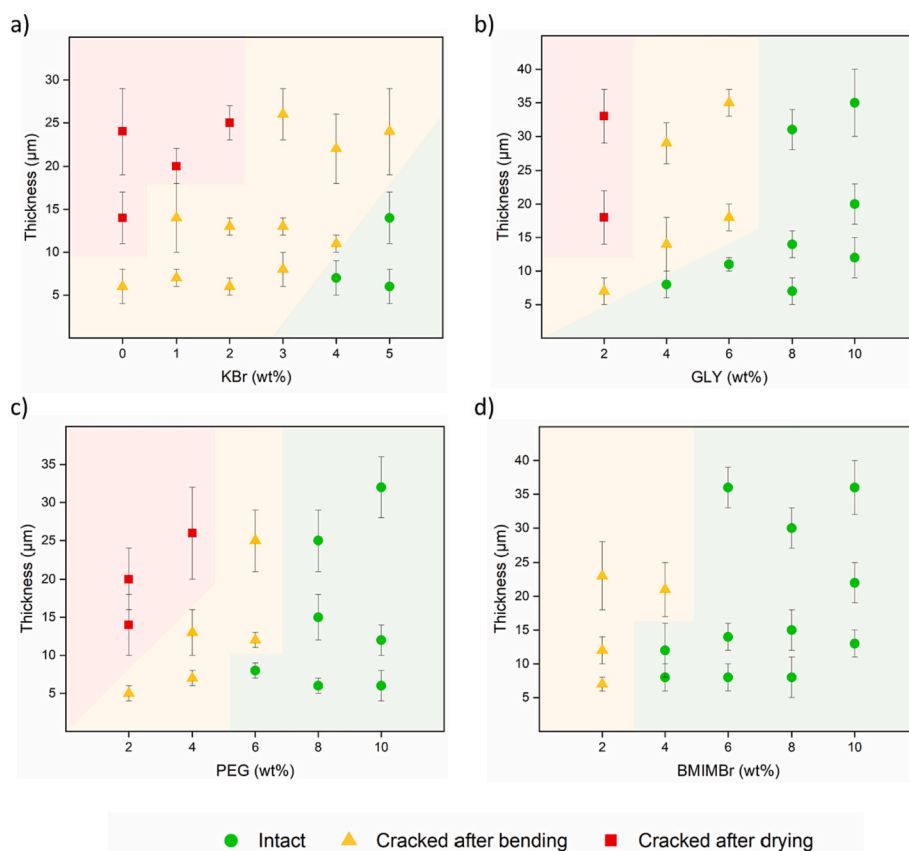


Fig. 5. State diagrams showing the cracking behavior during drying or after bending of films plasticized by different concentrations of: a) KBr, b) GLY, c) PEG, and d) BMIMBr. Different zones of cracking states are separated by colors. Error bars indicate the standard deviation in dry thickness; wt% indicates concentration in the initial wet films.

concentration, the samples were too soft to be removed from the substrate. Films containing >4 wt% OMIMBr showed such severe demixing that a homogeneous sample could not be prepared.

The mechanical properties of these films were assessed by comparing their Young's modulus, tensile strength, and elongation at break (Fig. 6). GLY and PEG both helped to plasticize the films, meaning that the Young's modulus and tensile strength decreased while the maximum elongation increased significantly with the increase of plasticizer concentration. When comparing GLY and PEG at the same wt%, GLY works more effectively, which has been observed also for other polymer films [67–71]. Smaller molecules can better penetrate between the polymer chains so that more plasticizer-polymer interactions can take place. Similarly, the smallest EMIMBr showed the most effective plasticizing effect among the three ILs. BMIMBr showed comparable plasticizing effect as GLY, even with better elongation. This again proves that ILs can loosen some ionic crosslinking of the network to allow more stretching. Another vital factor is the compatibility of hydrophilicity. The increasing alkyl chain length of the imidazolium not only increases the size, but also increases the hydrophobicity, making OMIMBr the least compatible in this hydrophilic system with the least degree of plasticization. Interestingly, this was also observed in a system where hydrophobic ILs, BMIMPF₆ and HMIMPF₆, were used to plasticize PVC. In this case, the more hydrophobic HMIMPF₆ showed better plasticization [72].

Representative stress-strain curves for all samples are summarized in Fig. S21. The gradual addition of plasticizers indeed led to a brittle-to-ductile transition of PEI/PSS. Moreover, the mechanical properties of BMIMBr plasticized films in two different thicknesses were compared (Fig. S22). The thicker films appeared more ductile with lower Young's modulus, lower tensile strength, and higher maximum elongation. Possibly, the thinner films were so difficult to handle that defects were

generated. Also, when peeling off 8 wt% BMIMBr plasticized thin samples, they were already stretched slightly. Another possibility can be that drying films with different thicknesses may cause different kinetics during film formation. This effect should be further investigated.

3.5.3. Effect of humidity

The effect of the relative humidity on the mechanical properties of the PEI/PSS films and its relation to plasticization with IL were investigated with dynamic mechanical analysis (DMA). Measurements were performed well within the linear viscoelastic regime as measured on dry films with amplitude sweeps. Sample fracture occurred well before any non-linearity could be observed (Fig. S23). The equilibration of the extensional storage modulus E' was monitored as a function of time while applying a single oscillatory frequency of 1 Hz. Samples were kept at ambient conditions (approx. 40 % RH), and equilibration to the applied RH clearly induced an increase in modulus at low RH, and a decrease in modulus at high RH. Representative equilibration curves are shown in Fig. S24 where it can be observed that samples were measured until E' reached a plateau. The plateau moduli were plotted as a function of RH in Fig. 7. Not all relative humidity were accessible for characterization since sample cracking can lead to fracture at low RH (below 30 %) while excessively high RH resulted in sample sagging due to plastic deformation (above 65 %). The equilibrium moduli clearly decreased with increasing RH. The plasticizing effect of ILs appears moderate at low RH. The response of E' to increasing RH, however, appears more dramatic for plasticized films, spanning several orders of magnitude, likely owing to the hydrophilicity of the ionic liquid. This trend is consistent with the swelling tests, where IL plasticized films showed significant expansion in water. While plasticization with ILs improves the mechanical performance at moderate RH, moisture resistance is not improved.

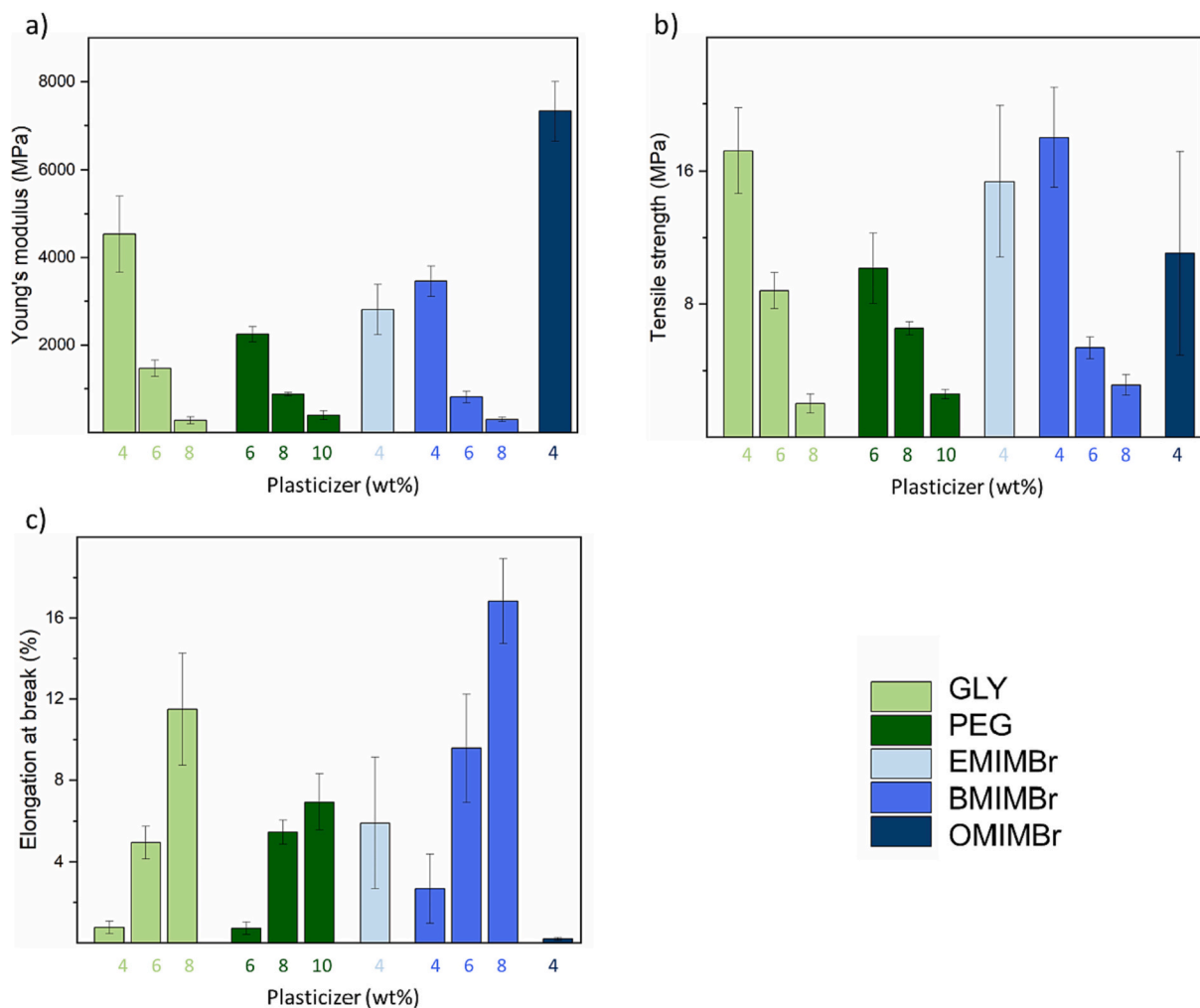


Fig. 6. a) Young's modulus, b) tensile strength, and c) elongation at break of plasticized samples with different concentrations.

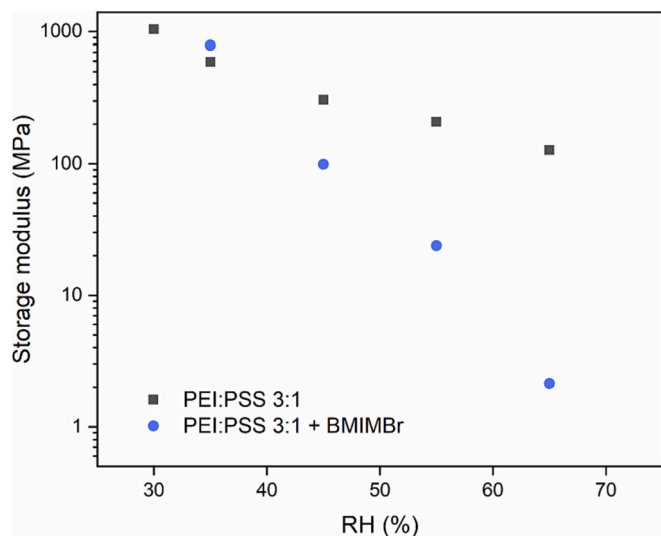


Fig. 7. Storage moduli of blank films and BMIMBr plasticized films (PEI:PSS at a ratio of 3:1) vs RH.

4. Conclusions

In this study, we have investigated various plasticizers for a PEI/PSS based polyelectrolyte complex coating. Our previous study [18] has shown that the strong ionic interaction is the main reason for their high degree of brittleness, instead of the chain entanglements. In summary (Fig. 8), the process to successfully prepare plasticized PEI/PSS films consists of two stages. Firstly, a homogenous solution should be formed. Selected polyols, salt, and amphiphilic ILs were all compatible within this aqueous system, while BMIMPF₆ was too hydrophobic which led to phase separation. After obtaining homogenous solutions, films were cast and during drying, solid plasticizers including SOR, KBr, and KPF₆ all showed crystallization. The absence of water initiated the recrystallization which caused opacity and poor plasticization. Dewetting/demixing behavior was observed for both EMIMBr and OMIMBr, which again shows the importance to balance the molecule size and hydrophilicity. GLY, PEG, EMIMBr, and BMIMBr showed effective plasticizing effects on a PEI/PSS polyelectrolyte complex film. GLY and PEG only act as lubricants among the chains, while amphiphilic ILs can reduce the ionic interactions between PEI and PSS. Thus, ILs can better improve the mechanical properties, and also have other advantages, such as lower vapor pressure and better thermal stability. Despite these improvements, the plasticizers used in this study cannot improve the water resistance of the hydrophilic PEI/PSS films, as shown by DMA. In the case of polyols, the majority of the added amount leached in water. For ILs, swelling happened in the form of expansion, while films were held

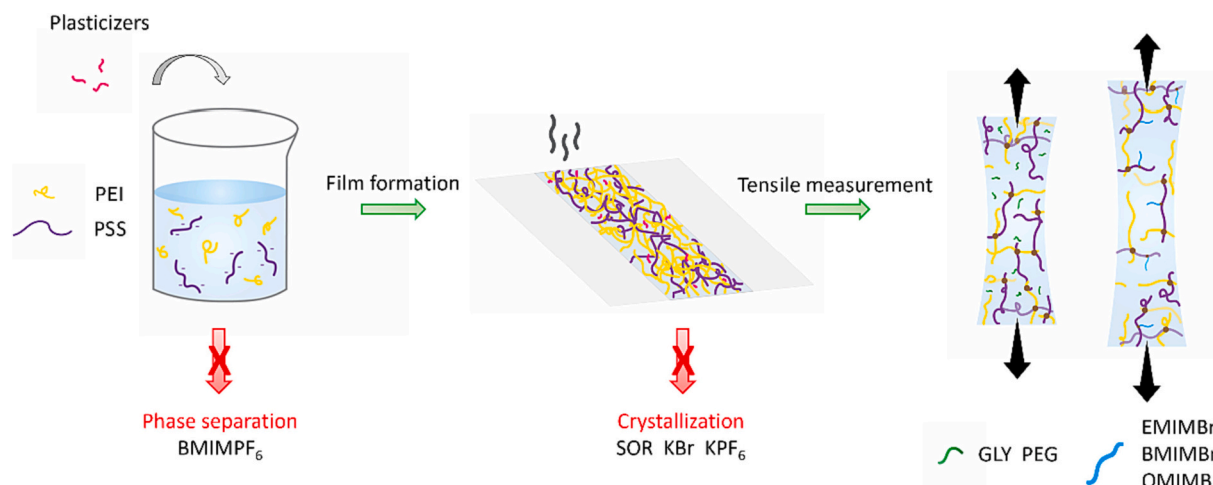


Fig. 8. Overview of all studied plasticizers. 1. Solution mixing: the plasticizers have to be hydrophilic enough to avoid phase separation. 2. Film formation: solid plasticizers tend to recrystallize due to drying and low water content. 3. The external ionic interactions between ILs and PEC help to better plasticize the films than polyols.

together by ionic interactions with less leaching.

For future work, the reproducibility and long-term stability of these plasticized films should be studied. Since the films remain hydrophilic, it is vital to study the recovery of the mechanical properties after exposed to extreme humidity/water. Meanwhile, there is still a gap in our understanding of the general film formation process, for example, how the film formation is influenced by film thickness and humidity. Further progress would require in situ characterizations of the dynamic processes during film formation and a systematic investigation of the different parameters that influence these processes. The adhesion of the applied coatings to various substrates was not studied here, but will be an important topic to pursue in the future.

CRediT authorship contribution statement

Jiaying Li: Investigation, Validation, Data curation, Writing – original draft.

Sophie van Lange: Investigation, Validation, Data curation, Writing – reviewing and editing.

Ameya Krishna B: Investigation, Validation, Data curation, Writing – reviewing and editing.

Anastasia Athanasiadou: Investigation, Validation, Data curation.

Gerard van Ewijk: Conceptualization, Writing – review and editing.

Derk Jan van Dijken: Conceptualization, Writing – review and editing.

Jasper van der Gucht: Conceptualization, Project administration, Funding acquisition, Writing – review and editing.

Wiebe M. de Vos: Conceptualization, Project administration, Funding acquisition, Supervision, Writing – review and editing.

Funding sources

This work is a part of Advanced Research Center for Chemical Building Blocks, ARC-CBBC, which is co-founded and co-financed by the Dutch Research Council (NWO) and the Netherlands Ministry of Economic Affairs and Climate.

Declaration of competing interest

The authors declare that they have no known competing financial interests or personal relationships that could have appeared to influence the work reported in this paper.

Data availability

Data will be made available on request.

Acknowledgment

This work was supported by ARC-CBBC.

Appendix A. Supplementary data

The document contains: 3-point bending measurement, pictures of solutions, KBr crystallization, calculation of KBr wt%, SOR crystallization, wrinkle formation of GLY/PEG plasticized films, phase separation of KPF₆/BMIMPF₆ plasticized films, dewetting/demixing behavior of EMIMBr/BMIMBr/OMIMBr plasticized films, FTIR spectra, SEM images, opacity of KPF₆/BMIMPF₆ plasticized films, water content measured by TGA/by weighing, water uptake, swelling in water, comparison of BMIMBr plasticized films in two different thicknesses, extra state diagrams of films, images of films after 3-point bending, thickness of measured tensile samples, representative stress-strain curves, amplitude sweep measurement, and raw DMA results. The Supporting Information is available free of charge. Supplementary data to this article can be found online at [doi:10.1016/j.porgcoat.2023.107459](https://doi.org/10.1016/j.porgcoat.2023.107459).

References

- [1] V.S. Meka, M.K.G. Sing, M.R. Pichika, S.R. Nali, V.R.M. Kolapalli, P. Kesharwani, A comprehensive review on polyelectrolyte complexes, *Drug Discov. Today* 22 (11) (2017) 1697–1706.
- [2] M. Haile, O. Sarwar, R. Henderson, R. Smith, J.C. Grunlan, Polyelectrolyte coacervates deposited as high gas barrier thin films, *Macromol. Rapid Commun.* 38 (1) (2017), 1600594.
- [3] J. Li, G. van Ewijk, D.J. van Dijken, J. van der Gucht, W.M. de Vos, Single-step application of polyelectrolyte complex films as oxygen barrier coatings, *ACS Appl. Mater. Interfaces* 13 (18) (2021) 21844–21853.
- [4] A.S. Michaels, Polyelectrolyte complexes, *Ind. Eng. Chem.* 57 (10) (1965) 32–40.
- [5] Q. Wang, J.B. Schlenoff, Tough strained fibers of a polyelectrolyte complex: pretensioned polymers, *RSC Adv.* 4 (87) (2014) 46675–46679.
- [6] P. Schaaf, J.B. Schlenoff, Saloplastics: processing compact polyelectrolyte complexes, *Adv. Mater.* 27 (15) (2015) 2420–2432.
- [7] M. Tirrell, Polyelectrolyte complexes: fluid or solid? *ACS Cent. Sci.* 4 (5) (2018) 532–533.
- [8] R.M. Hodge, T.J. Bastow, G.H. Edward, G.P. Simon, A.J. Hill, Free volume and the mechanism of plasticization in water-swollen poly(vinyl alcohol), *Macromolecules* 29 (25) (1996) 8137–8143.
- [9] P. Batys, Y. Zhang, J.L. Lutkenhaus, M. Sammalkorpi, Hydration and temperature response of water mobility in poly(diallyldimethylammonium)-poly(sodium 4-styrenesulfonate) complexes, *Macromolecules* 51 (20) (2018) 8268–8277.

- [10] M. Bocqué, C. Voirin, V. Lapinte, S. Caillol, J.-J. Robin, Petro-based and bio-based plasticizers: chemical structures to plasticizing properties, *J. Polym. Sci. A Polym. Chem.* 54 (1) (2016) 11–33.
- [11] H.H. Hariri, A.M. Lehaf, J.B. Schlenoff, Mechanical properties of osmotically stressed polyelectrolyte complexes and multilayers: water as a plasticizer, *Macromolecules* 45 (23) (2012) 9364–9372.
- [12] J. Fu, R.L. Abbott, H.M. Fares, J.B. Schlenoff, Water and the glass transition temperature in a polyelectrolyte complex, *ACS Macro Lett.* 6 (10) (2017) 1114–1118.
- [13] Y. Chen, M. Yang, J.B. Schlenoff, Glass transitions in hydrated polyelectrolyte complexes, *Macromolecules* 54 (8) (2021) 3822–3831.
- [14] S. Manoj Lalwani, C.I. Eneh, J.L. Lutkenhaus, Emerging trends in the dynamics of polyelectrolyte complexes, *Phys. Chem. Chem. Phys.* 22 (42) (2020) 24157–24177.
- [15] J.B. Schlenoff, H. Ly, M. Li, Charge and mass balance in polyelectrolyte multilayers, *J. Am. Chem. Soc.* 120 (30) (1998) 7626–7634.
- [16] Q. Wang, J.B. Schlenoff, The polyelectrolyte complex/coacervate continuum, *Macromolecules* 47 (9) (2014) 3108–3116.
- [17] R. Zhang, Y. Zhang, H.S. Antila, J.L. Lutkenhaus, M. Sammalkorpi, Role of salt and water in the plasticization of PDAC/PSS polyelectrolyte assemblies, *J. Phys. Chem. B* 121 (1) (2017) 322–333.
- [18] J. Li, B.A. Krishna, G. van Ewijk, D.J. van Dijken, W.M. de Vos, J. van der Gucht, A comparison of complexation induced brittleness in PEI/PSS and PEI/NaPSS single-step coatings, *Colloids Surf. A Physicochem. Eng. Asp.* 648 (2022), 129143.
- [19] Y. Sun, C. Meng, Y. Zheng, Y. Xie, W. He, Y. Wang, K. Qiao, L. Yue, The effects of two biocompatible plasticizers on the performance of dry bacterial cellulose membrane: a comparative study, *Cellulose* 25 (10) (2018) 5893–5908.
- [20] M. Rico, S. Rodríguez-Llamazares, L. Barral, R. Bouza, B. Montero, Processing and characterization of polyols plasticized-starch reinforced with microcrystalline cellulose, *Carbohydr. Polym.* 149 (2016) 83–93.
- [21] S.D. Pasini Cabello, E.A. Takara, J. Marchese, N.A. Ochoa, Influence of plasticizers in pectin films: microstructural changes, *Mater. Chem. Phys.* 162 (2015) 491–497.
- [22] B. Ucpinar Durmaz, A. Aytac, Effects of polyol-based plasticizer types and concentration on the properties of polyvinyl alcohol and casein blend films, *J. Polym. Environ.* 29 (1) (2021) 313–322.
- [23] M. Liu, Y. Zhou, Y. Zhang, C. Yu, S. Cao, Preparation and structural analysis of chitosan films with and without sorbitol, *Food Hydrocoll.* 33 (2) (2013) 186–191.
- [24] V. Epure, M. Griffon, E. Pollet, L. Averous, Structure and properties of glycerol-plasticized chitosan obtained by mechanical kneading, *Carbohydr. Polym.* 83 (2) (2011) 947–952.
- [25] V. Jost, K. Kobsik, M. Schmid, K. Noller, Influence of plasticiser on the barrier, mechanical and grease resistance properties of alginate cast films, *Carbohydr. Polym.* 110 (2014) 309–319.
- [26] C. Gao, E. Pollet, L. Averous, Properties of glycerol-plasticized alginate films obtained by thermo-mechanical mixing, *Food Hydrocoll.* 63 (2017) 414–420.
- [27] F. Bagheri, M. Radi, S. Amiri, Drying conditions highly influence the characteristics of glycerol-plasticized alginate films, *Food Hydrocoll.* 90 (2019) 162–171.
- [28] P. Treenate, P. Monvisade, M. Yamaguchi, The effect of glycerol/water and sorbitol/water on the plasticization of hydroxyethylacryl chitosan/sodium alginate films, *MATEC Web Conf.* 30 (2015) 02006.
- [29] H.E. Salama, M.S. Abdel Aziz, M.W. Sabaa, Novel biodegradable and antibacterial edible films based on alginate and chitosan biguanidine hydrochloride, *Int. J. Biol. Macromol.* 116 (2018) 443–450.
- [30] N. Joseph, P. Ahmadiannamini, R. Hoogenboom, I.F.J. Vankelecom, layer-by-layer preparation of polyelectrolyte multilayer membranes for separation, *Polym. Chem.* 5 (6) (2014) 1817–1831.
- [31] R.F. Shamoun, A. Reisch, J.B. Schlenoff, Extruded saloplastic polyelectrolyte complexes, *Adv. Funct. Mater.* 22 (9) (2012) 1923–1931.
- [32] E.N. Durmaz, S. Sahin, E. Virga, S. de Beer, L.C.P.M. de Smet, W.M. de Vos, Polyelectrolytes as building blocks for next-generation membranes with advanced functionalities, *ACS Appl. Polym. Mater.* 3 (9) (2021) 4347–4374.
- [33] J. Ren, W. Zhang, F. Lou, Y. Wang, W. Guo, Characteristics of starch-based films produced using glycerol and 1-Butyl-3-methylimidazolium chloride as combined plasticizers, *Starch - Stärke* 69 (1–2) (2017), 1600161.
- [34] M.P. Scott, C.S. Brazel, M.G. Benton, J.W. Mays, J.D. Holbrey, R.D. Rogers, Application of ionic liquids as plasticizers for poly(methyl methacrylate), *Chem. Commun.* 13 (2002) 1370–1371.
- [35] J. Wang, Y. Liang, Z. Zhang, C. Ye, Y. Chen, P. Wei, Y. Wang, Y. Xia, Thermoplastic starch plasticized by polymeric ionic liquid, *Eur. Polym. J.* 148 (2021), 110367.
- [36] R. Leones, F. Sentanin, S.C. Nunes, J.M.S.S. Esperança, M.C. Gonçalves, A. Pawlicka, V.D.Z. Bermudez, M.M. Silva, Effect of the alkyl chain length of the ionic liquid anion on polymer electrolytes properties, *Electrochim. Acta* 184 (2015) 171–178.
- [37] X. Li, A. Qin, X. Zhao, B. Ma, C. He, The plasticization mechanism of Polyacrylonitrile/1-Butyl-3-methylimidazolium chloride system, *Polymer* 55 (22) (2014) 5773–5780.
- [38] A. Sankri, A. Arhaliass, I. Dez, A.C. Gaumont, Y. Grohens, D. Lourdin, I. Pillin, A. Rolland-Sabaté, E. Leroy, Thermoplastic starch plasticized by an ionic liquid, *Carbohydr. Polym.* 82 (2) (2010) 256–263.
- [39] M. Rahman, C.S. Brazel, Ionic liquids: new generation stable plasticizers for poly(vinyl chloride), *Polym. Degrad. Stab.* 91 (12) (2006) 3371–3382.
- [40] A. Bendaoud, Y. Chalamet, Plasticizing effect of ionic liquid on cellulose acetate obtained by melt processing, *Carbohydr. Polym.* 108 (2014) 75–82.
- [41] J. Wu, J. Bai, Z. Xue, Y. Liao, X. Zhou, X. Xie, Insight into glass transition of cellulose based on direct thermal processing after plasticization by ionic liquid, *Cellulose* 22 (1) (2015) 89–99.
- [42] Z. Jin, S. Wang, J. Wang, M. Zhao, Effects of plasticization conditions on the structures and properties of cellulose packaging films from ionic liquid [BMIM]Cl, *J. Appl. Polym. Sci.* 125 (1) (2012) 704–709.
- [43] S.S. Hilva, J.F. Mano, R.L. Reis, Ionic liquids in the processing and chemical modification of chitin and chitosan for biomedical applications, *Green Chem.* 19 (5) (2017) 1208–1220.
- [44] K. Wilpizewska, T. Spychaj, Ionic liquids: media for starch dissolution, plasticization and modification, *Carbohydr. Polym.* 86 (2) (2011) 424–428.
- [45] N. Parveen, M. Schönhoff, Swelling and stability of polyelectrolyte multilayers in ionic liquid solutions, *Macromolecules* 46 (19) (2013) 7880–7888.
- [46] N. Parveen, P.K. Jana, M. Schönhoff, Viscoelastic properties of polyelectrolyte multilayers swollen with ionic liquid solutions, *Polymers (Basel)* 11 (8) (2019) 1285.
- [47] B. Zhang, D.A. Hoagland, Z. Su, Ionic liquids as plasticizers for polyelectrolyte complexes, *J. Phys. Chem. B* 119 (8) (2015) 3603–3607.
- [48] B.S. Tomar, A. Shahin, M.S. Tirumkudulu, Cracking in drying films of polymer solutions, *Soft Matter* 16 (14) (2020) 3476–3484.
- [49] J.N. Sarmousakis, M.J.D. Low, The solubility of potassium hexafluorophosphate in water, *J. Am. Chem. Soc.* 77 (24) (1955) 6518–6519.
- [50] D.S.H. Wong, J.P. Chen, J.M. Chang, C.H. Chou, Phase equilibria of water and ionic liquids [EMIM][PF6] and [BMIM][PF6], *Fluid Phase Equilib.* 194–197 (2002) 1089–1095.
- [51] H.M. Fares, Y.E. Ghoussoub, J.D. Delgado, J. Fu, V.S. Urban, J.B. Schlenoff, Scattering neutrons along the polyelectrolyte complex/coacervate continuum, *Macromolecules* 51 (13) (2018) 4945–4955.
- [52] A.F. Miller, Exploiting wrinkle formation, *Science* 317 (5838) (2007) 605–606.
- [53] J. Rodríguez-Hernández, Wrinkled interfaces: taking advantage of surface instabilities to pattern polymer surfaces, *Prog. Polym. Sci.* 42 (2015) 1–41.
- [54] B.R. Machado, S.P. Facchi, A.C. de Oliveira, C.S. Nunes, P.R. Souza, B.H. Vilinski, K.C. Popat, M.J. Kipper, E.C. Muniz, A.F. Martins, Bactericidal pectin/chitosan/glycerol films for food pack coatings: a critical viewpoint, *Int. J. Mol. Sci.* 21 (22) (2020) 8663.
- [55] N.E. Suyatma, L. Tighzert, A. Copinet, V. Coma, Effects of hydrophilic plasticizers on mechanical, thermal, and surface properties of chitosan films, *J. Agric. Food Chem.* 53 (10) (2005) 3950–3957.
- [56] J.R. Rodríguez-Núñez, T.J. Madera-Santana, D.I. Sánchez-Machado, J. López-Cervantes, H. Soto Valdez, Chitosan/hydrophilic plasticizer-based films: preparation, physicochemical and antimicrobial properties, *J. Polym. Environ.* 22 (1) (2014) 41–51.
- [57] C. Caicedo, C.A. Díaz-Cruz, E.J. Jiménez-Regalado, R.Y. Aguirre-Loredo, Effect of plasticizer content on mechanical and water vapor permeability of maize starch/PVOH/chitosan composite films, *Materials (Basel, Switzerland)* 15 (4) (2022).
- [58] A. Domján, J. Bajdik, K. Pintye-Hódi, Understanding of the plasticizing effects of glycerol and PEG 400 on chitosan films using solid-state NMR spectroscopy, *Macromolecules* 42 (13) (2009) 4667–4673.
- [59] M.L. Castelló, J. Dweck, D.A.G. Aranda, Thermal stability and water content determination of glycerol by thermogravimetry, *J. Therm. Anal. Calorim.* 97 (2) (2009) 627.
- [60] V.Y. Mena-Cervantes, R. Hernández-Altamirano, A. Tiscareño-Ferrer, Development of a green one-step neutralization process for valorization of crude glycerol obtained from biodiesel, *Environ. Sci. Pollut. Res.* 27 (23) (2020) 28500–28509.
- [61] A. Zarour, S. Omar, R. Abu-Reziq, Preparation of poly(ethylene glycol)@Polyurea microcapsules using Oil/Oil emulsions and their application as microreactors, *Polymers (Basel)* 13 (15) (2021) 2566.
- [62] Y. Yu, J. Mai, L. Wang, X. Li, Z. Jiang, F. Wang, Ship-in-a-bottle synthesis of amine-functionalized ionic liquids in nay zeolite for CO₂ capture, *Sci. Rep.* 4 (1) (2014) 5997.
- [63] Q. Su, Y. Qi, X. Yao, W. Cheng, L. Dong, S. Chen, S. Zhang, Ionic liquids tailored and confined by one-step assembly with mesoporous silica for boosting the catalytic conversion of CO₂ into cyclic carbonates, *Green Chem.* 20 (14) (2018) 3232–3241.
- [64] N.B. Shirsath, G.R. Gupta, V.V. Gite, J.S. Meshram, Studies of thermally assisted interactions of polysulphide polymer with ionic liquids, *Bull. Mater. Sci.* 41 (2) (2018) 63.
- [65] I.H.J. Arellano, J.G. Guarino, F.U. Paredes, S.D. Arco, Thermal stability and moisture uptake of 1-Alkyl-3-methylimidazolium bromide, *J. Therm. Anal. Calorim.* 103 (2) (2011) 725–730.
- [66] S.K. Yedla, B. Velaga, S. Choudhury, A. Namdeo, A.K. Golder, N.R. Peela, 1-Butyl-3-methylimidazolium bromide functionalized zeolites: nature of interactions and catalytic activity for carbohydrate conversion to platform chemicals, *React. Chem. Eng.* 5 (9) (2020) 1738–1750.
- [67] T. Bourtoom, Plasticizer effect on the properties of biodegradable blend film from rice starch-chitosan, *Songklanakarin J. Sci. Technol.* (2008) 30.
- [68] J. Tarique, S.M. Sapuan, A. Khalina, Effect of glycerol plasticizer loading on the physical, mechanical, thermal, and barrier properties of arrowroot (Maranta Arundinacea) starch biopolymers, *Sci. Rep.* 11 (1) (2021) 13900.
- [69] P. Jantrawit, T. Chaiwarit, K. Jantanasakulwong, C.H. Brachais, O. Chambin, Effect of plasticizer type on tensile property and in vitro indomethacin release of thin films based on low-methoxyl pectin, *Polymers (Basel)* 9 (7) (2017) 289.
- [70] V.C.-H. Wan, M.S. Kim, S.-Y. Lee, Water vapor permeability and mechanical properties of soy protein isolate edible films composed of different plasticizer combinations, *J. Food Sci.* 70 (6) (2005) e387-e391.
- [71] M.G.A. Vieira, M.A. da Silva, L.O. dos Santos, M.M. Beppu, Natural-based plasticizers and biopolymer films: a review, *Eur. Polym. J.* 47 (3) (2011) 254–263.
- [72] L.X. Hou, S. Wang, Study on ionic liquid [BMIM]PF₆ and [HMIM]PF₆ as plasticizer for PVC paste resin, *Polym. Bull.* 67 (7) (2011) 1273–1283.